Supporting Information

Achieving Over 30% Photon-to-Photon Efficiency with Tandem OLED Structures in Organic Upconversion Devices

Xingwei Han[1], Jiayue Han[1,2], Meiyu He[1], Chao Han[1],Lei Guo[1], He Yu[1,2], Jun Gou[1,2], Jun Wang[1,2]*

[1]School of Optoelectronic Science and Engineering, University of Electronic Science and Technology of China, Chengdu 610054, China

[2]State Key Laboratory of Electronic Thin Films and Integrated Devices, University of Electronic Science and Technology of China, Chengdu 610054, China

* Corresponding author. E-mail: wjun@uestc.edu.cn

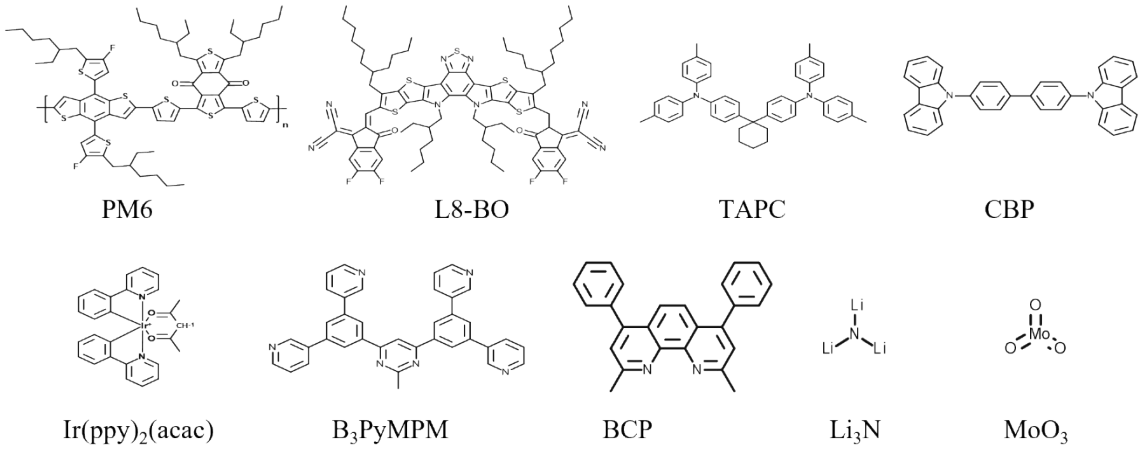

Figure S1. The molecular structures of the materials utilized in this work.

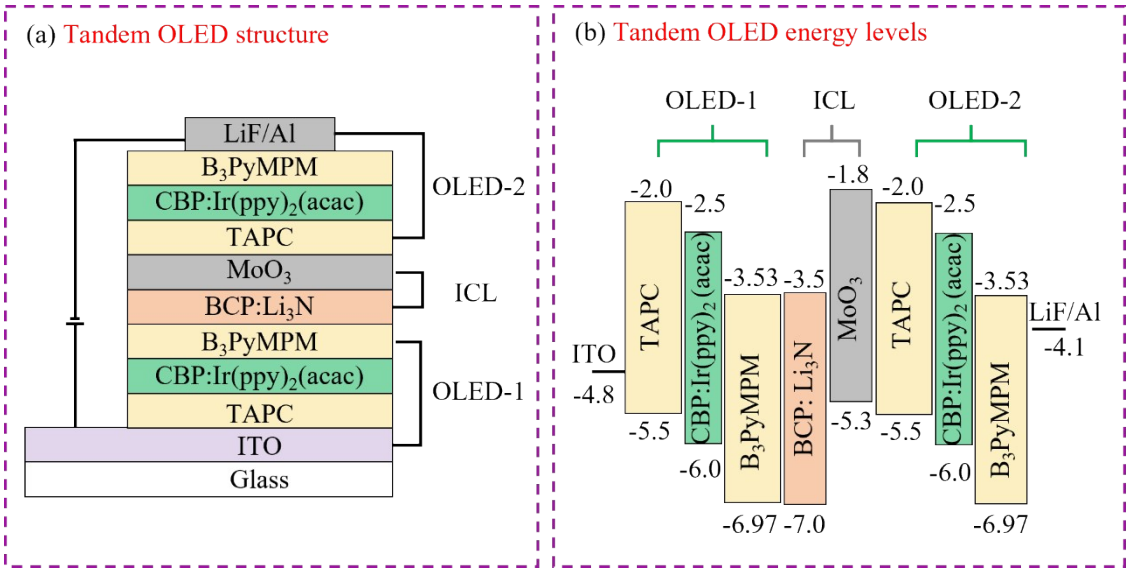

Figure S2. Tandem OLED structure and principles. (a) Schematic diagram of the structure; (b) Energy level diagram.

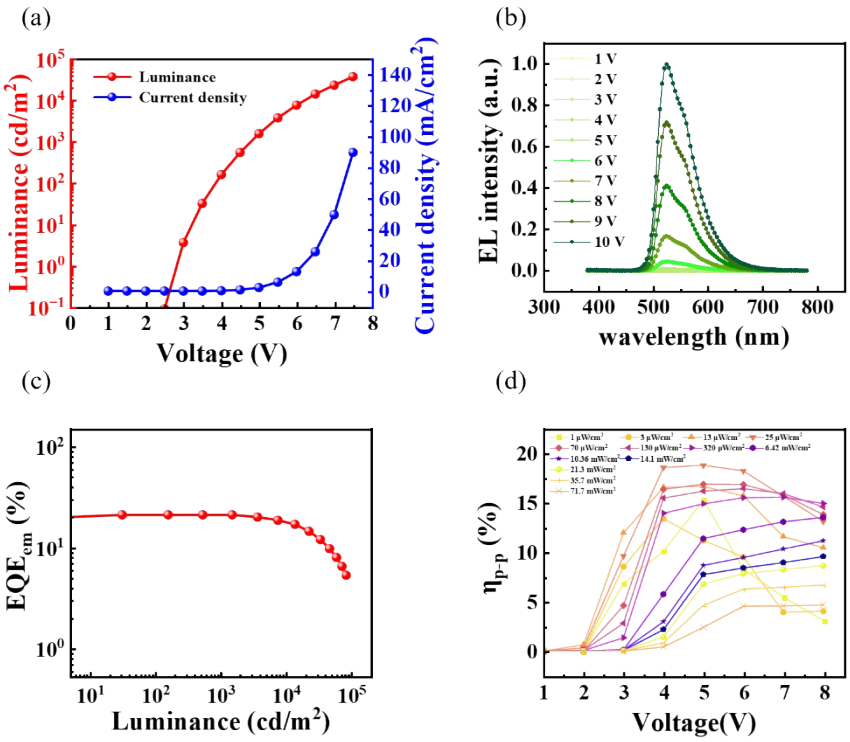

Figure S3. Performance of single OLED. (a) J-V-L characteristic curves of a single OLED; (b) Electroluminescence spectra at different bias voltages; (c) EQE_{em} at various luminance levels; (d) η_{p-p} of the OUD based on a single OLED.

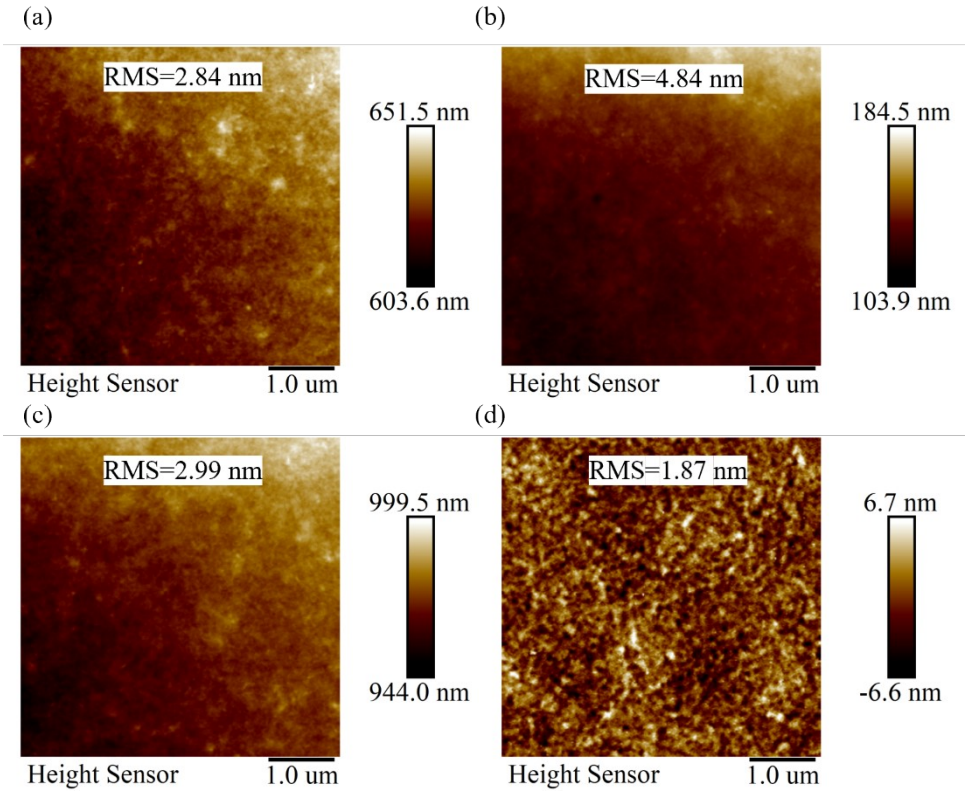

Figure S4. AFM characterization of film surfaces. (a) OLED-1 film; (b) OLED-1/BCP:Li_3N/MoO_3 film; (c) OLED-1/BCP:Li_3N/MoO_3/OLED-2 film; (d) standalone PM6:L8-BO film.

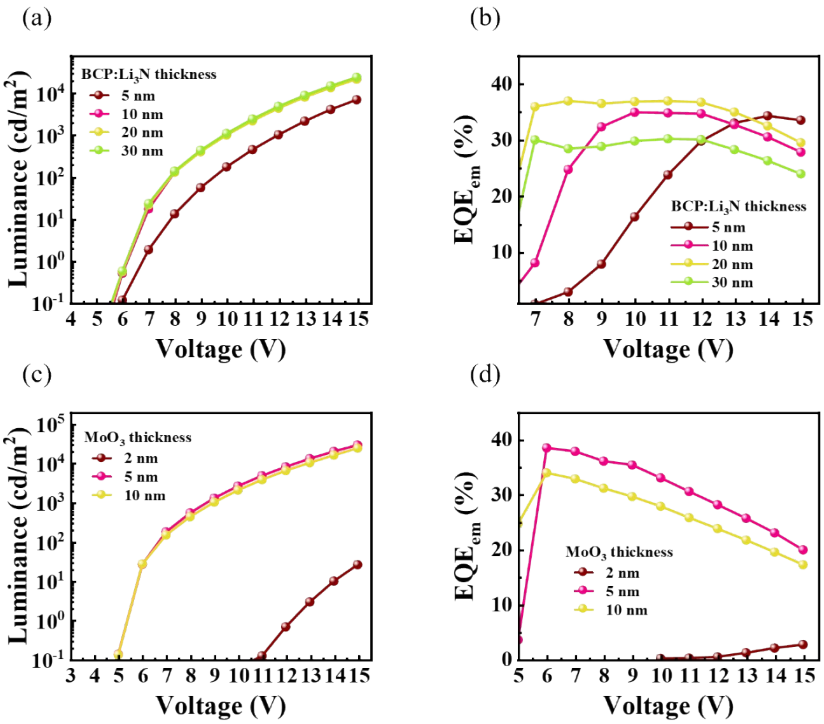

Figure S5. Impact of ICL thickness on tandem OLED performance. (a) Effect of BCP:Li_3N layer thickness on luminance; (b) Effect of BCP:Li_3N layer thickness on EQE_{em}; (c) Effect of MoO_3 layer thickness on luminance; (d) Effect of MoO_3 layer thickness on EQE_{em}.

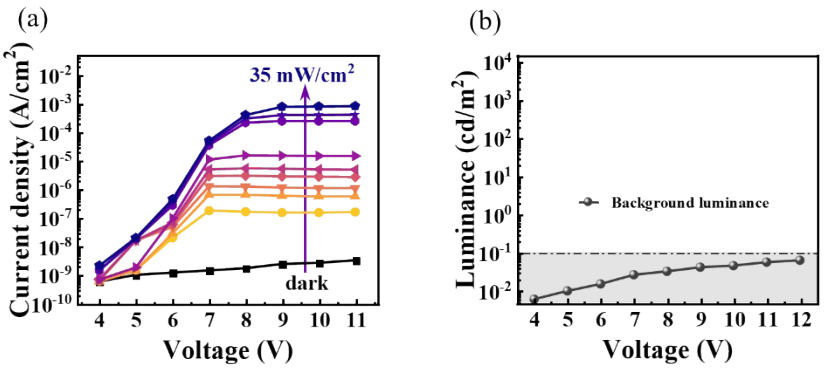

Figure S6. (a) J-V characteristics under different incident light power densities; (b) Background luminance under different bias voltages

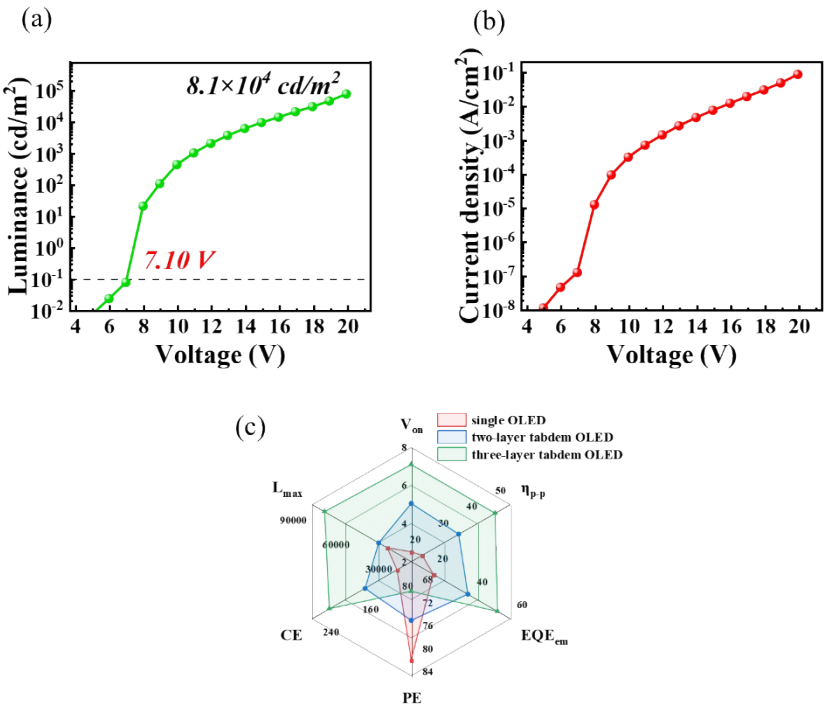

Figure S7. Performance characterization of the three-layer tandem OLED. (a) L-V characteristics; (b) J-V characteristics. (c) The performance comparison of devices with different numbers of tandem OLEDs.

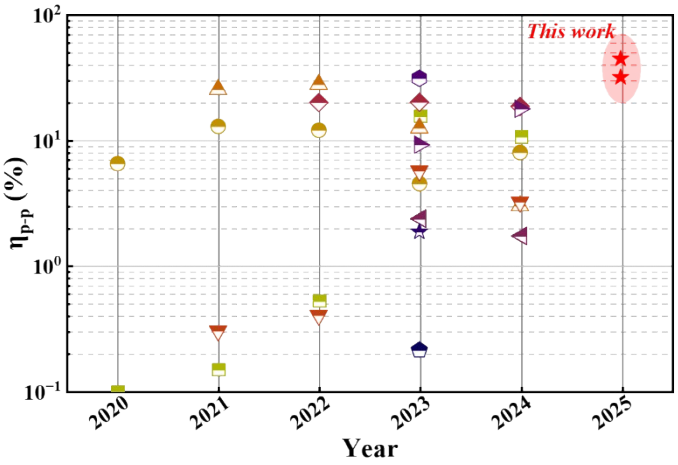

Figure S8. Comparison of η_{p-p} for upconversion devices over the past five years.

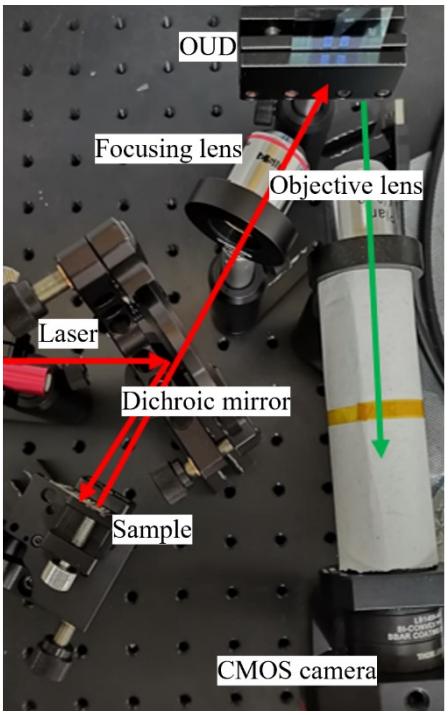

Figure S9. Practical optical path for upconversion imaging of infrared reflected light from samples.